GENETIC ANALYSIS OF MESANGIAL MATRIX EXPANSION IN AGING MICE AND IDENTIFICATION OF *FAR2* AS A CANDIDATE GENE

Gerda A. Noordmans
Christina R. Caputo
Yuan Huang
Susan M. Sheehan
Marian Bulthuis
Peter Heeringa
Jan-Luuk Hillebrands
Harry van Goor
Ron Korstanje

Journal of the American Society of Nephrology 2013; 24(12): 1995-2001

ABSTRACT

Aging of the kidney is associated with renal damage, in particular mesangial matrix expansion (MME). To unravel the mechanisms of aging it is important to identify genes involved in this process, since this might help to design novel therapeutic modalities aimed at prevention and regression. In this study, structural changes in glomeruli of 24 mouse inbred strains were characterized in male mice at 6, 12, and 20 months of age. Haplotype association mapping was used to determine genetic loci associated with the presence of MME at 20 months. This analysis identified a significant association with a 200-Kb haplotype block on Chromosome 6 containing *Far2*. Sequencing revealed that the strains with MME contain a 9-bp sequence in the 5´UTR of *Far2*, which is absent in most of the strains without MME. Real-time PCR showed a two-fold increase in the expression of *Far2* in the kidneys of strains with the insert compared to strains without the insert, and subsequent cloning of the two allelic forms of the 5´UTR of *Far2* into a luciferase reporter vector showed that this sequence difference causes the difference in *Far2* expression. Overexpression of *Far2* in a mouse mesangial cell line induces upregulation of platelet activating factor and the fibrotic marker transforming growth factor β. *Far2* catalyzes the reduction of fatty acyl-CoA to fatty alcohols, a possible precursor of platelet activating factor, and upregulation causes an increase in the factors that induce MME. This is a novel pathway involved in renal aging.

INTRODUCTION

Renal aging is associated with a decline in renal structure and function, making the elderly more vulnerable for superimposed stress such as hypertension, diabetes, or acute kidney injury [1,2]. Eventually, renal aging may lead to chronic kidney disease, and ultimately, treatment with dialysis or transplantation might be needed. Chronic kidney disease is a major health problem, especially regarding the growing geriatric population [3].

The aging kidney shows functional changes such as decreased glomerular filtration rate, reduced sodium homeostasis, and morphological changes in glomeruli, tubuli, and interstitium [4]. A characteristic feature of glomerular aging is the mesangial accumulation of extracellular matrix (ECM) proteins, which usually precedes glomerulosclerosis [3,5]. The mesangial cell is cardinal for glomerular function through its close interaction with both endothelial cells and podocytes [6]. Mesangial matrix expansion (MME) might be caused by nephron loss and subsequent hyperfiltration in the functional nephrons. This may result in local glomerular hypertension and compensatory hypertrophy, which are thought to lead to cytokine and growth factor-mediated MME and, eventually, glomerulosclerosis [3].

The normal mesangium contains several ECM proteins, including collagen type IV, V and VI; fibronectin; and proteoglycans [6,7]. MME is believed to result from an imbalance between synthesis of ECM components and decreased ECM degradation by matrix metalloproteinases that are under the control of specific inhibitors [8]. Several growth-promoting factors are involved in this process, but an important promoter of ECM accumulation is TGFβ [9,10]. An age-related increase in TGFβ has been shown in the rat kidney in addition to an increase in age-related structural changes such as glomerulosclerosis, mesangial matrix expansion, and interstitial fibrosis [11]. Different pathways seem to play a role in age-related kidney damage, and although sex and genetic background seem to be of high importance, specific genes that contribute to age-related damage of the kidney still remain to be identified [4].

Mice are an ideal species for studying the genetics of aging since they have a relatively short lifespan and share 99% of their genes with humans [12,13]. With the availability of large numbers of mouse inbred strains, haplotype association mapping (HAM) can be readily performed to identify associations between the phenotype and the haplotypes of mouse inbred strains [14]. Recently, several genes involved in the age-related susceptibility for albuminuria have been identified in various strains of mice based on albumin-to-creatinine ratios (ACR) [15]. ACR, however, has limitations since it is a quantitative phenotype with an unequal distribution among individuals and it is far downstream of the disease cascade. In this study we characterized MME in the kidneys of 24 inbred strains

in male mice at 20 months of age, using HAM to identify genes associated with MME in these aged mice.

MATERIALS & METHODS

Mice and tissue collection

Groups of 30 males from each of 24 different inbred strains (Table 1) were obtained from The Jackson Laboratory, Bar Harbor, ME. Mice were housed in a climate-controlled facility with a 12-hour:12-hour light-dark cycle and provided free access to food and water throughout the experiment. After weaning, mice were maintained on a chow diet (LabDiet® 5K52, PMI Nutritional International, Bentwood, Mo). Ten males from each strain were sacrificed at 6, 12, and 20 months of age and both kidneys were collected. Kidneys were not perfused because of the collection of blood and other tissues in the same experiment. The left kidney was flash frozen in liquid nitrogen and stored at −80°C, while the right kidney was fixed in Bouin's fixative, followed by embedding in paraffin. All experiments were approved by The Jackson Laboratory's Animal Care and Use Committee.

Histological staining and scoring

Periodic acid-Schiff (PAS) staining was performed on 3-µm paraffin sections. PAS staining was used for morphological evaluation. Histological scoring was performed in a blinded manner. For each animal, 50 glomeruli were scored for the presence or absence of mesangial matrix expansion (MME). A glomerulus was marked as positive for mesangial matrix expansion if the mesangium was broadened more than twice. For each individual animal, a score was given of percentage of affected glomeruli. Per strain, the mean of 6 animals was calculated, representing the percentage of affected glomeruli and the standard deviation is given to depict the variation within one strain. The threshold for accounting a strain as positive for MME was set at 10% of affected glomeruli. This cut-off point was chosen because the three-dimensional structure of the glomerulus always accounts for some false positive-scoring in tissue sections.

Haplotype association mapping

Haplotype association mapping for MME was performed using the free R add-on package EMMA (efficient mixed models association; http://mouse.cs.ucla.edu/emma), which uses a linear mixed model algorithm to control for population structure and genetic relatedness [20]. The strain mean was used as phenotype input and the analysis was conducted using a panel of 623,124 SNPs from the Mouse Diversity Genotyping Array, a high-density mouse genotyping array that has captured the known genetic variation present in the laboratory mouse

Table 1. Characteristics of the 24 mouse inbred strains used in this study.

Strain	Presence of MME	*Far2* insertion/deletion
BALB/cByJ	y	ins
C57BL/6J	y	ins
C57BL/10J	y	ins
C57BR/cdJ	y	ins
CBA/J	y	ins
KK/J	y	ins
NOD.B10Sn-H2b/J	y	ins
NON/LtJ	y	ins
NZW/LacJ	y	ins
P/J	y	ins
SM/J	y	ins
MRL/J	y	ins
129S1/SvImJ	n	ins
PWD/PHJ	n	ins
RIIIS/J	n	ins
C57L/J	n	ins
WSB/EiJ	n	ins
C3H/HeJ	n	del
C57BLKS/J	n	del
DBA/2J	n	del
FVB/NJ	n	del
LP/J	n	del
SWR/J	n	del
BTBR T+ tf/J	n	del

[21]. Non-informative SNPs (i.e. SNPs that were not polymorphic between the strains used in our study) were removed from this data set, which resulted in a total of 274,648 informative SNPs. Each SNP was evaluated individually and a P-value was recorded as the strength of the genotype-phenotype association. All P-values were transformed using –log10 (P-value) in the scan plot. Genome sequences within the candidate regions were compared between the different strains based on their haplotype distribution using the Sanger Institute's mouse genome databases.

Real-time PCR of *Far2*

RNA was isolated from kidney samples using the Trizol method. Samples were diluted and 2 µg was used for cDNA synthesis using the QuantiTect RT kit (Qiagen). Renal mRNA levels for *Far2* were determined using a primer set designed by Primerdesign Ltd (Southampton, UK) (forward: 5´-GGGTTGGGTTGATAATCTAAATGG-3´, reverse: 5´-GGAATCACATCTGCCACTGC-3´). Real-time PCR was performed using the 7900 HT Sequence Detection System (Applied Biosystems, Inc., Foster City, CA, USA) with SYBR green. mRNA levels were expressed relative to those of the beta-2 microglobulin gene (B2m).

Cloning of the *Far2* 5´UTR indel into pGL4.10 and transfection of mesangial cells

To clone the 5´UTR 9-bp indel of *Far2*, restriction site-containing 5´UTR regions of *Far2* were synthesized by Aldevron for both the 9-bp insertion and the 9-bp deletion. Synthesized oligos were subsequently restriction digested and ligated into separate pGL4.10 vectors (named pGL4.10-ins and pGL4.10-del). Mesangial cells (MES-13) isolated from (C57Bl/6J x SJL/J)F1 mice transgenic for the early region of simian virus 40 and mouse liver NMu3Li cells were obtained from ATTC [22]. $1.0*10^6$ MES-13 cells/mL were seeded into 1 mL of serum containing 3:1 DMEM-Ham's F12 media and incubated for 24 hours at 37°C. Dual transfection was done with pGL4.10-ins or pGL4.10-del and pGL4.73 using FuGene HD transfection reagent (Promega) in a 3.0 µL per 2.0 µg plasmid ratio. Following a 48-hour incubation in serum free media, cells were lysed via Dual Luciferase Reporter Assay System (Promega) and cell extract was collected for each sample. Each cell extract was transferred into a separate well and activated using a luciferase assay substrate (Promega). Firefly luciferase and Renilla luciferase counts per second (CPS) were determined on a Victor 3 multi-label plate reader. The relative luciferase expression was calculated by dividing firefly luminescense CPS by Renilla luminescense CPS.

Cloning of *Far2* cDNA into pCMV6 and transfection of mesangial cells

The *Far2* cDNA pCMV6 vector construct was kindly provided by Dr. D.W. Russell [16]. The plasmid was prepared for transfection into mesangial cells. $1.0*10^6$ MES-13 cells/mL were seeded into 1 mL of serum containing 3:1 DMEM-Ham's F12 media and incubated for 24 hours at 37°C. Following incubation, a transient transfection was done using pCMV6-m*Far2* plasmid and FuGene HD transfection reagent at a 2.0 µg per 3 µL ratio. A similar transfection was done using pCMV6-XL control plasmid. Following incubation, media was collected for ELISA studies, protein was collected and processed by scraping into RIPA buffer, and tissues were collected in lysis buffer for RNA studies. Samples were collected at 24-, 48-, and 72-hour incubation times. Platelet Activating Factor levels were measured using a K-assay

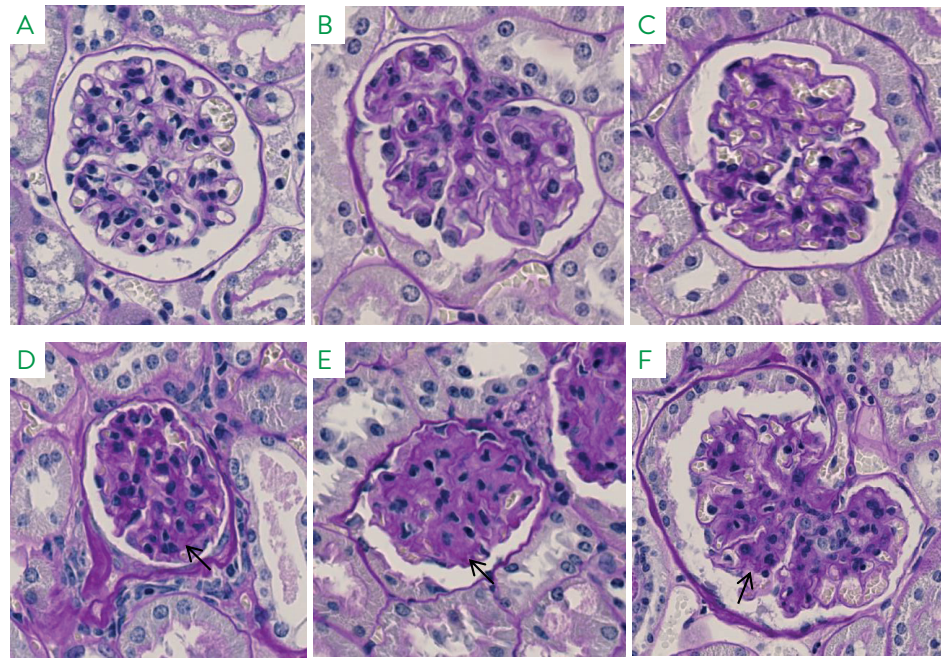

Figure 1. Representative example of morphological changes on PAS staining. *A-C. Glomerulus of a 20-month old male mouse without MME, LP/J (A), SWR (B) and WSB (C). D-F. Glomerulus of a male NZW/LacJ (D), KK (E) and SM (F) mouse with MME. Broadened mesangium (arrow).*

Mus musculus ELISA kit (USCN) and immuno-active TGF-B1 levels were measured using a mouse TGF-B1 DuoSet ELISA development kit (R&D biosystems).

RESULTS

Strains with mesangial matrix expansion

Histological analysis was performed for males of all strains from The Jackson Laboratory Shock Center cross-sectional study (agingmice.jax.org/) that survived until 20 months of age and for which kidneys were available. On a PAS staining, scoring of 50 glomeruli for the presence or absence of MME was performed for each animal. (Figure 1). The threshold for accounting a strain as positive for MME was set at 10% (5 out of 50) of affected glomeruli. Analysis of glomeruli at 6 months of age in strains that did not develop MME at later time points also resulted in an average of 1-2 affected glomeruli using the criteria describe above. We considered these glomeruli as false positive; the three-dimensional structure of the glomerulus may always account for some false positive scoring in tissue sections.
Based on this we decided to set the relatively high threshold of 10% to prevent inclusion of false positive strains that would obscure our genetic analysis, and only

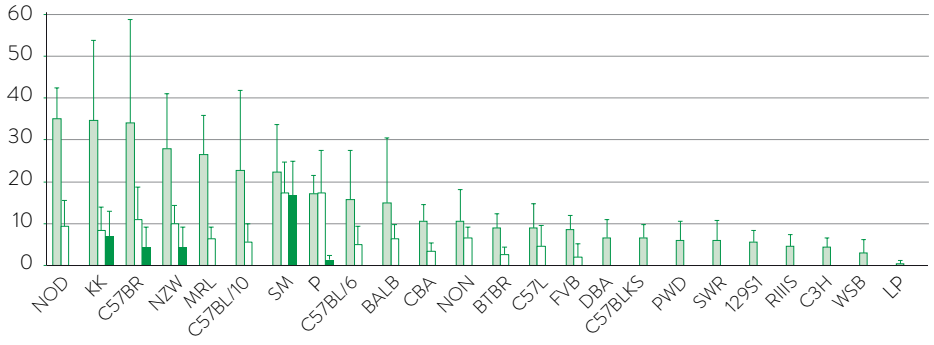

Figure 2. Strain and age-dependent increase in matrix accumulation. *For each strain the mean percentage and standard deviation of affected glomeruli is shown at 20 (light green bar), 12 (white bar), and 6 months (dark green bar) of age. Scoring at a younger time point was only performed if the threshold of 10% was reached at the 20-month time point. At each time point, n=6, except for P at 12 months (n=3).*

include strains which we considered having moderate to severe MME. Strains with an average of <5 affected glomeruli at 20 months of age were considered negative for MME. Twelve out of 24 strains showed MME at 20 months of age (Table 1). Strains that were positive for MME or above the threshold of 10 percent at 20 months were also evaluated at 12 months of age. At 6 months of age, only the 5 strains that were positive for MME or close to the threshold at 12 months of age were evaluated. Figure 2 demonstrates the variation of MME between the strains and the variation within a strain over time.

Haplotype association mapping identified *Far2*

A panel of 623,124 SNPs was used for the haplotype association mapping. After removing the non-informative SNPs, analysis was carried out with a total of 274,648 SNPs. For each SNP the association between genotype and MME phenotype was analyzed individually and a P-value was recorded as the strength of the genotype-phenotype association (Figure 3). To identify the most significant association with MME, we focused on the peak with the lowest P-value and identified a 200-Kb haplotype block (between rs32310749 and rs30560187) on Chromosome (Chr) 6, which is different between those strains with MME and those strains without MME. According to the Ensembl Genome Browser (NCBI m37 assembly), *Far2* is the only gene within this haplotype block (Figure 4A).

By comparing genome sequencing within this region using the Sanger Institute Mouse Genomes Project database (www.sanger.ac.uk/resources/mouse/genomes/), we identified a 9-bp sequence (CTCGAGTGC) in the 5´UTR *Far2* (encoded by exon 1 (ENSMUSE00000860810) according to Ensembl) that is present in all strains with MME but absent in most strains without MME, such as

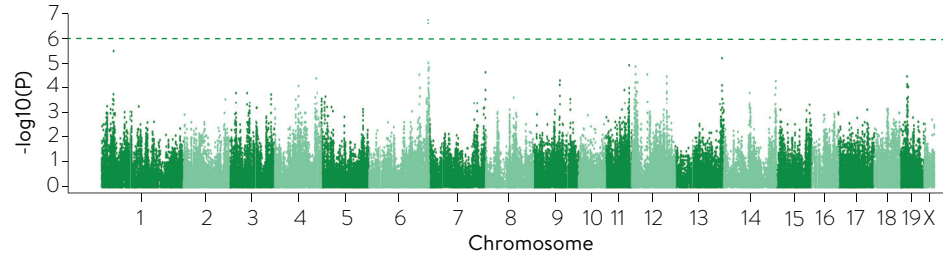

Figure 3. Genome-wide scan for MME. *The significant threshold was set to $P < 10^{-6}$.*

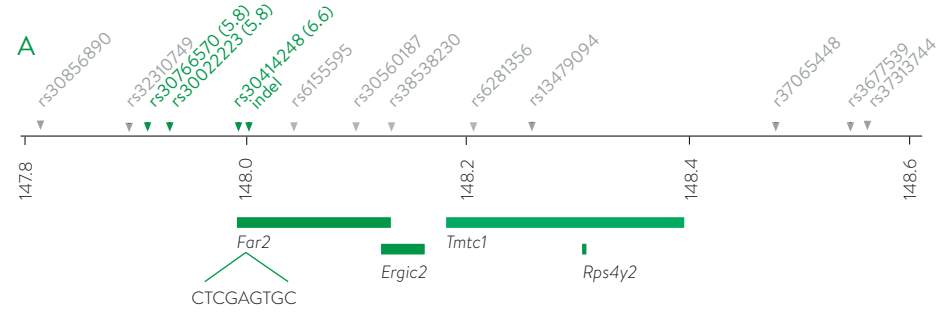

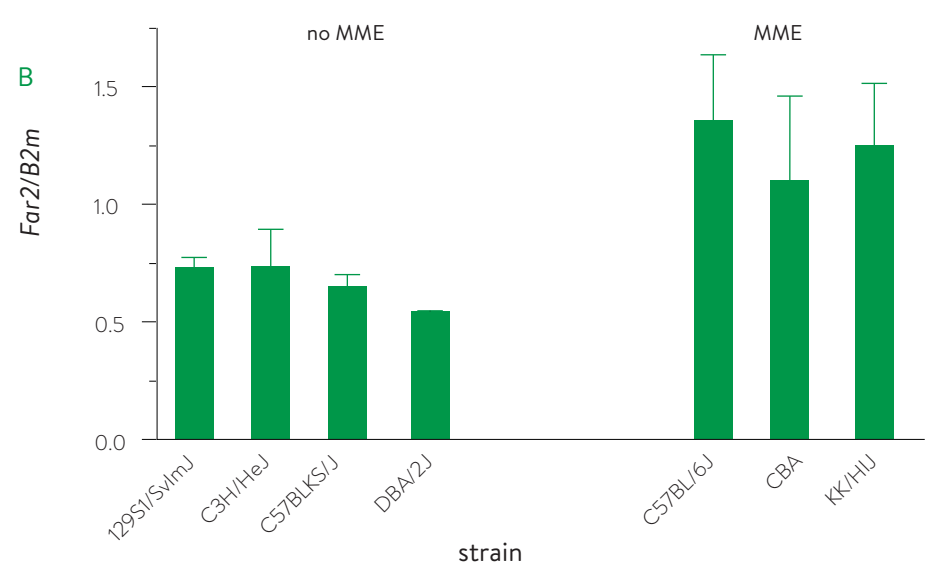

Figure 4. Association and expression of *Far2*. *A. The haplotype block between rs32310749 and rs30560187 is associated with MME. The only gene found in this region is Far2. The 9-bp sequence CTCGAGTGC is absent in 7 out of 11 strains without MME. B. Far2 expression levels correlate with MME. The results represent the mean ± SEM. Comparing all animals (regardless of strain) with and without MME using a t-test showed a significant difference ($P < 0.01$).*

DBA/2J and C3H/HeJ (Figure 4A). We designed primers flanking this region and sequenced all strains used in our study. All strains with MME contain the 9-bp sequence insertion, while 7 out of 12 of the strains without MME do not (Table 1).

Far2 expression associates with MME

To determine whether this polymorphism has an effect on gene expression, we designed primers for real-time PCR and measured the renal expression of *Far2* in five strains without MME and three strains with MME. We observed a two-fold higher expression of *Far2* in the strains with MME compared to the strains without MME (Figure 4B).

The 9-bp indel in the 5´UTR of *Far2* causes the difference in *Far2* expression

Both alleles of the *Far2* 5´UTR were synthesized and cloned into pGL4.10 in front of the luc2 luciferase gene (Figure 5A). The plasmids were co-transfected with pGL4.73 containing the hRluc luciferase into SV40 MES-13 (mesangial) cells and NMu3Li (mouse liver) cells. The luc2 luciferase expression was divided by the hRluc luciferase expression. Luciferase activity was measured as an indicator of expression. Comparing the construct containing the deletion to the construct with the insertion, a significant increase in the relative luciferase expression was demonstrated for the allele with the 9-bp insert in both cell types (Figure 5B).

Far2 overexpression causes upregulation of PAF and TGFβ

Transfection of a mouse mesangial cell line (MES 13) with the entire C57BL/6J *Far2* cDNA (ENSMUST00000111607) (containing the insert) cloned into a pCMV6 vector was performed to determine if *Far2* overexpression leads to an increase in production of PAF and fibrosis promoting factor TGFβ. Both the production of PAF ($P < 0.05$) and TGFβ ($P < 0.02$) was significantly upregulated in the media of cells transfected with the *Far2* plasmid compared to the media of cells transfected with the empty control plasmid (Figure 6).

DISCUSSION

Using haplotype association mapping, this study identified a small locus on Chr 6 that is associated with age-related mesangial matrix expansion and contains the *Far2* gene. All strains with MME contained a 9-bp sequence insertion in the 5´UTR of *Far2* that is absent in 7 of the 12 strains without MME. The insertion might disrupt a transcription factor binding site, but our gel mobility shift assays failed to show a shift after incubation with cell lysate (data not shown). We found a two-fold higher renal expression of *Far2* in strains with MME compared to strains with no MME. Although all strains with MME have the insertion, there is not a complete

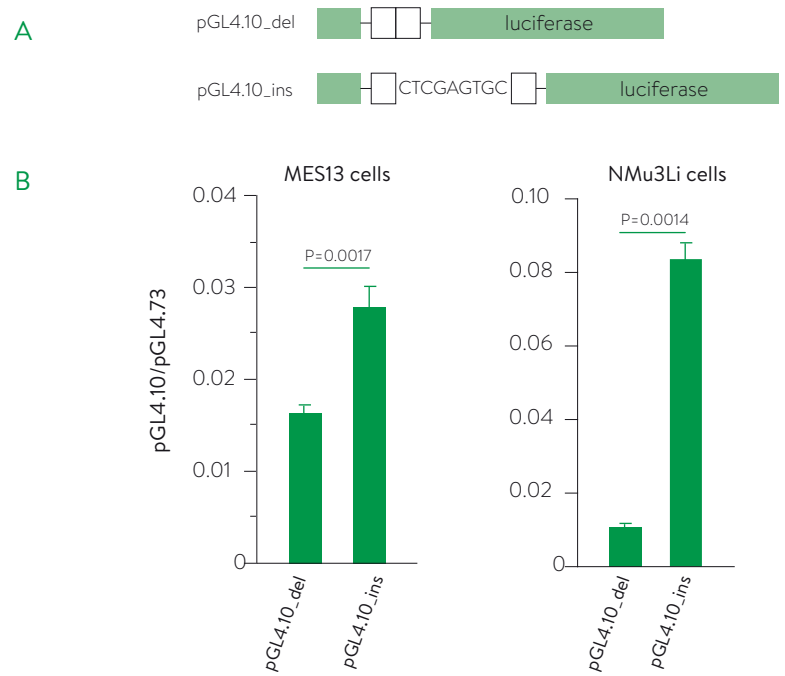

Figure 5. The 9-bp indel in the promoter region of *Far2* influences gene expression. *A. Both alleles of the 5´UTR of Far2 were cloned in front of the luciferase gene of pGL4.10 and co-transfected with 4.73 into MES 13 mesangial cells and NMu3Li liver cells. B. Relative luciferase expression in the allele with the 9-bp insert is significantly higher compared to the allele without the insert. The results represent the mean ± SEM.*

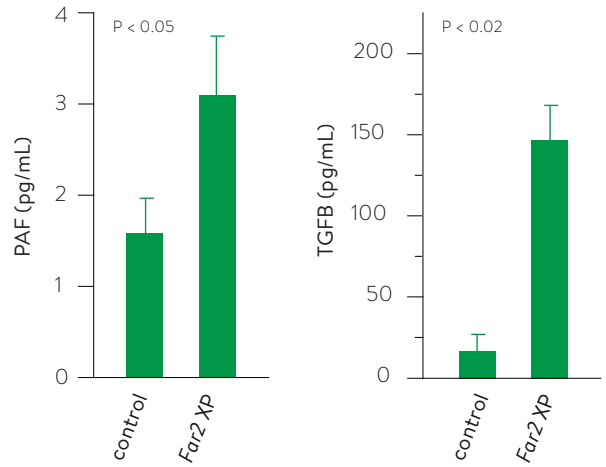

Figure 6. *Far2* overexpression causes upregulation of PAF and TGFβ. *PAF protein levels are significantly upregulated in the media of MES-13 cells transfected with pCMV6-Far2 compared to the media of cells transfected with pCMV6 control vector ($P < 0.05$). The expression of TGFβ is also significantly increased in the cells overexpressing Far2 compared to the control ($P < 0.02$).*

correlation between the presence of the 9-bp sequence and MME. The 129S1, RIIIS, WSB, C57L/J, and PWD strains have the 9-bp insertion, while we did not observe MME above our threshold of 10% in their kidneys. If we assume that this insertion is the causative difference, we would expect these strains to develop MME. Thus, it is likely that other loci on the genome affect MME and that these strains might have alleles at these other loci that counteract the *Far2* allele. By cloning the 5´UTR of the two different alleles into an expression vector, we showed that this sequence difference is causing a change in luciferase expression and therefore very likely to also cause the difference in *Far2* expression in most strains.

Far2 encodes the protein Fatty Acyl-CoA Reductase 2, which is localized in the peroxisome. *Far2* catalyzes the reduction of fatty acyl-CoA to fatty alcohols. We hypothesize that these fatty alcohols are the precursors of platelet activating factor (PAF) [16], a potent inflammatory mediator that activates platelets, neutrophils, eosinophils and macrophages. PAF also participates in the pathogenesis of proteinuria and glomerular damage, probably through changing the glomerular permselectivity, although its exact role is still unknown [17]. A study using platelet-activating factor receptor (PAFR)-deficient mice showed the involvement of PAF in folic acid-induced renal injury. These mice showed amelioration of interstitial fibrosis and reduced macrophage infiltration, indicating the involvement of PAF in the pathogenesis of chronic interstitial fibrosis [17]. In response to exogenous stimulations, PAF is produced by a variety of cells such as neutrophils, eosinophils, monocytes, mesangial cells, and by the renal medulla and cortex [18]. Exposure of cultured rat and human mesangial cells to PAF stimulates the gene expression and synthesis of the matrix proteins fibronectin and type IV collagen [19]. To test our hypothesis we transfected mouse MES-13 mesangial cells with a plasmid overexpressing *Far2* cDNA and could demonstrate that PAF production was upregulated. We also show that *Far2* overexpression is causing a significant upregulation of TGFβ. TGFβ is a pro-fibrotic cytokine that greatly stimulates the accumulation of extracellular matrix by several mechanisms. It directly stimulates the production of matrix proteins like fibronectin, collagens, and proteoglycans. On the other hand, it also inhibits degradation of matrix by inhibiting the production of matrix metalloproteinases (MMPs) and stimulating the production of tissue inhibitors of metalloproteinases (TIMPs) [9].

Upregulation of PAF and TGFβ in response to *Far2* overexpression suggests that intervening in the expression or activation of *Far2* would reduce MME and consequently delay renal aging. However, it must be mentioned that little is known about the specific functions of *Far2* in mammals. Therefore blocking or inhibiting the expression of *Far2* might have unknown consequences. Interventions further downstream of *Far2* might influence matrix accumulation more specifically. However, the exact pathway through which *Far2* increases PAF and TGFβ is unknown.

By unraveling the mechanism of kidney aging, we aim to develop novel strategies to intervene in the process of renal aging. To our knowledge this is the first study to identify a novel gene involved in MME through induction of PAF and TGFβ, both of which are involved in the pathogenesis of sclerosis. Further experiments focusing on the modulation of the *Far2*/PAF/TGFβ-pathway should be performed to understand and eventually delay aging of the kidney.

ACKNOWLEDGEMENTS

We thank Jesse Hammer for preparation of the figures.

FUNDING

This work was funded by the University of Groningen Graduate School of Medical Sciences (GAN), GM076468 from the National Institute of General Medical Sciences (R.K.), and AG038070 from National Institute on Aging (R.K.), and the National Cancer Institute Cancer Core grant (CA034196) to The Jackson Laboratory.

REFERENCES

1. Lindeman RD, Tobin J, Shock NW. Longitudinal studies on the rate of decline in renal function with age. J Am Geriatr Soc. 1985;33: 278-285.

2. Rifkin DE, Coca SG, Kalantar-Zadeh K. Does AKI truly lead to CKD? J Am Soc Nephrol. 2012;23: 979-984.

3. Zhou XJ, Rakheja D, Yu X, Saxena R, Vaziri ND, Silva FG. The aging kidney. Kidney Int. 2008;74: 710-720.

4. Martin JE, Sheaff MT. Renal ageing. J Pathol. 2007;211: 198-205.

5. Baylis C, Corman B. The aging kidney: Insights from experimental studies. J Am Soc Nephrol. 1998;9: 699-709.

6. Schlondorff D, Banas B. The mesangial cell revisited: No cell is an island. J Am Soc Nephrol. 2009;20: 1179-1187.

7. Mason RM, Wahab NA. Extracellular matrix metabolism in diabetic nephropathy. J Am Soc Nephrol. 2003;14: 1358-1373.

8. Ronco P, Chatziantoniou C. Matrix metalloproteinases and matrix receptors in progression and reversal of kidney disease: Therapeutic perspectives. Kidney Int. 2008;74: 873-878.

9. Border WA, Noble NA. TGF-beta in kidney fibrosis: A target for gene therapy. Kidney Int. 1997;51: 1388-1396.

10. Roberts AB, McCune BK, Sporn MB. TGF-beta: Regulation of extracellular matrix. Kidney Int. 1992;41: 557-559.

11. Ruiz-Torres MP, Bosch RJ, O'Valle F, Del Moral RG, Ramirez C, Masseroli M, et al. Age-related increase in expression of TGF-beta1 in the rat kidney: Relationship to morphologic changes. J Am Soc Nephrol. 1998;9: 782-791.

12. Boguski MS. Comparative genomics: The mouse that roared. Nature. 2002;420: 515-516.

13. Yuan R, Peters LL, Paigen B. Mice as a mammalian model for research on the genetics of aging. ILAR J. 2011;52: 4-15.

14. Tsaih SW, Korstanje R. Haplotype association mapping in mice. Methods Mol Biol. 2009;573: 213-222.

15. Tsaih SW, Pezzolesi MG, Yuan R, Warram JH, Krolewski AS, Korstanje R. Genetic analysis of albuminuria in aging mice and concordance with loci for human diabetic nephropathy found in a genome-wide association scan. Kidney Int. 2010;77: 201-210.

16. Cheng JB, Russell DW. Mammalian wax biosynthesis. I. identification of two fatty acyl-coenzyme A reductases with different substrate specificities and tissue distributions. J Biol Chem. 2004;279: 37789-37797.

17. Doi K, Okamoto K, Negishi K, Suzuki Y, Nakao A, Fujita T, et al. Attenuation of folic acid-induced renal inflammatory injury in platelet-activating factor receptor-deficient mice. Am J Pathol. 2006;168: 1413-1424.

18. Ishii S, Shimizu T. Platelet-activating factor (PAF) receptor and genetically engineered PAF receptor mutant mice. Prog Lipid Res. 2000;39: 41-82.

19. Ruiz-Ortega M, Largo R, Bustos C, Gomez-Garre D, Egido J. Platelet-activating factor stimulates gene expression and synthesis of matrix proteins in cultured rat and human mesangial cells: Role of TGF-beta. J Am Soc Nephrol. 1997;8: 1266-1275.

20. Kang HM, Zaitlen NA, Wade CM, Kirby A, Heckerman D, Daly MJ, et al. Efficient control of population structure in model organism association mapping. Genetics. 2008;178: 1709-1723.

21. Yang H, Ding Y, Hutchins LN, Szatkiewicz J, Bell TA, Paigen BJ, et al. A customized and versatile high-density genotyping array for the mouse. Nat Methods. 2009;6: 663-666.

22. MacKay K, Striker LJ, Elliot S, Pinkert CA, Brinster RL, Striker GE. Glomerular epithelial, mesangial, and endothelial cell lines from transgenic mice. Kidney Int. 1988;33: 677-684.